



ChemComm

Time Evolution of Moduli of a Polymer-Induced Liquid-Precursor (PILP) of Calcium Carbonate

Journal:	<i>ChemComm</i>
Manuscript ID	CC-COM-01-2024-000449.R1
Article Type:	Communication

SCHOLARONE™
Manuscripts

Time Evolution of Moduli of a Polymer-Induced Liquid Precursor (PILP) of Calcium Carbonate

Received 00th January 20xx,
Accepted 00th January 20xx

Changyu Shao,^{a, b, f} Haihua Pan,^{*b} Jinhui Tao,^c Kang Rae Cho,^{d, e} Ruikang Tang,^{*f} Laurie B. Gower,^g
and James J. De Yoreo^{*c}

DOI: 10.1039/x0xx00000x

In situ AFM observations show that when PILP droplets contact a surface, their initial properties are either a liquid with a high interfacial tension (350 mJ/m²) or a soft gel-like material with a low modulus (less than 0.2 MPa). These findings suggest that PILP may initially be liquid-like to infiltrate collagen fibrils, enabling the production of interpenetrating composites, and/or become viscoelastic, to provide a means for moulding minerals.

Crystallization is the primary process by which molecules condense into an ordered structure. Monomer-by-monomer attachment is the scenario envisioned in classical crystallization models. However, recent experimental findings indicated the existence of more intricate crystallization pathways, involving intermediates consisting of multi-ion clusters,^{1, 2} amorphous precursors,³ nanoparticles,^{4, 5} or even dense liquids.⁶⁻⁸ Moreover, the introduction of polyionic polymers, both biological and synthetic origin, has been demonstrated to stabilize amorphous states and generate a polymer-induced liquid precursor (PILP) phase in various mineral systems, such as calcium carbonate,⁷ calcium phosphate,⁹ and barium carbonate.¹⁰

The notion of PILP as a mouldable precursor to a mineral phase has attracted significant attention within the biomineralization community due to the ubiquitous proteins

that are rich in acidic side groups (carboxylate, phosphate, sulfate), the visual similarity of PILP droplets to mineral precursors formed during both biomineralization and biomimetic synthesis,^{11, 12} and the potential ability of PILP to be formed into a variety of non-equilibrium (i.e., non-faceted) morphologies, such as crystal “drops”,⁷ thin films/tablets,¹³ fibers,¹⁰ and crystals shaped within templates.¹⁴ With regard to the liquid-like property, the mineral precursor has been shown to infiltrate the nanoscale compartments in macromolecular matrices, which is a common theme in biominerals. This has been observed, for example, in the *in vitro* intrafibrillar mineralization of collagen fibrils, which Olszta *et al.* hypothesized to occur through the capillary action of the fluidic droplets.⁸

Although the concept of amorphous precursors stabilized by polyionic polymers has gained widespread acceptance, the liquid nature of PILP has remained a subject of contention. The initial PILP paper presented compelling optical evidence for liquid-like behavior, a finding subsequently supported by NMR studies of self-diffusion and relaxation times.¹⁵ However, the crystalline products that formed from the PILP particles exhibited a colloidal texture, and although the colloids were very densely packed and appeared to fully coalesce into monolithic crystals, the remnant texture of the PILP precursors suggested that PILP particles do not flow like a liquid. Whether or not PILP is a true liquid or a soft solid, the elastic modulus and surface tension are key to understanding its wetting, flow, and moulding properties, but they have not been measured, despite their significance.¹⁶

In this study, we conducted a comprehensive analysis of the time-dependent mechanical response of PILP under deformation using *in situ* atomic force microscopy (AFM). Our results demonstrate that the PILP has a mechanical response characteristic of a gel-like material, which exhibits an increase in stiffness with time. However, it is important to note that our results do not rule out the potential that PILP may initially exhibit true liquid behavior prior to its interaction with a surface.

^a Stomatology Hospital, School of Stomatology, Zhejiang University School of Medicine, Clinical Research Center for Oral Diseases of Zhejiang Province, Key Laboratory of Oral Biomedical Research of Zhejiang Province, Cancer Center of Zhejiang University, Hangzhou, 310006, China

^b Qiushi Academy for Advanced Studies, Zhejiang University, Hangzhou, 310027, China

^c Physical Sciences Division, Pacific Northwest National Laboratory, WA, 99354, USA

^d Molecular Foundry, Lawrence Berkeley National Laboratory, CA, 94720, USA

^e Department of Applied Chemistry, College of Engineering, Cheongju University, Cheongju 28503, Republic of Korea

^f Centre for Biomaterials and Biopathways and Department of Chemistry, Zhejiang University, Hangzhou, 310027, China

^g Department of Materials Science & Engineering, University of Florida, FL, 32611, USA

† Electronic Supplementary Information (ESI) available: Experimental sections, supported Figures, Supported text. See DOI: 10.1039/x0xx00000x

Using polyacrylic acid sodium salt (PAA-5k) as a stabilizer for PILP formation (see Experiment section, ESI†), agglomerated droplets were formed on a silicon wafer from a calcium carbonate solution during the free drift of supersaturation (Fig. S1, ESI†). The precipitates appeared to be partially merged droplets/particles with morphologies strongly reminiscent of those formed when viscous liquid droplets merge together and partially spread on a surface into a reticulated film. However, these agglomerates did not form a smooth and completely continuous film (as observed in Gower and Odom's conditions⁷), suggesting a more rapid evolution in the PILP's mechanical properties, as the droplets may have dehydrated and solidified when becoming exposed to the open-air conditions. With progressive aging, vaterite crystals nucleated and grew into spherulitic aggregates at the expense of the (dissolving) precursor film of PILP (Fig. S2, ESI†).

In this experiment, the free drift of the supersaturation is driven by the release of CO₂ in open-air conditions (25°C and 60% relative humidity). This drift can be greatly slowed by partially sealing the solution in a container to retard the release of CO₂, as was done in our AFM experiments. After depositing an aliquot of the initial solution on a silicon wafer, it was immediately transferred to the liquid cell of the AFM, which has an O-ring seal. After sealing, approximately 100 μL of additional calcium carbonate solution was injected to completely fill the liquid cell. The initial precipitates were then observed by *in-situ* AFM.

Unfortunately, the earliest stages of PILP formation and/or deposition could not be captured by AFM due to an inherent characteristic of the measurement technique. The formation of PILP particles in the initial solution resulted in the scattering of the laser beam used to detect the deflection of the AFM probe, which in turn led to an unstable signal from the position-

sensitive photodiode used to record that deflection. As a result, no images could be acquired and no forces could be measured until the PILP particles had settled out of solution after about 25 min. Therefore, our results only pertain to the properties of PILP after that initial period.

In contrast to what was observed in open-air conditions, PILP in sealed solutions did not form large (micro-sized) agglomerated droplets. Instead, the PILP consisted of discrete structures ranging from about 10 to 100 nm in diameter (Fig. 1a), with a roughly Gaussian height distribution and a mean height of only 6 nm, presumably because the small volume of the fluid cell results in too little PILP to produce significant agglomeration. The shallow height of the larger droplets relative to the particle dimensions, even if they represent agglomerated droplets, suggests that the precursor was able to partially wet the surface in the early stage of formation. Over time, the distribution coarsened, with small deposits shrinking and eventually disappearing (see circles in Fig. 1a), while large deposits grew, leading to a clear bimodal height distribution (Fig. 1b). Thus the size evolution appears to reflect Ostwald ripening, rather than the direct coalescence of small droplets. The latter process was not possible in these experiments, because the PILP deposits were firmly attached to the silicon surface by the time imaging was possible, and Brownian motion did not occur. Consequently, even after 5 h the PILP remained in the form of discrete nanoscale deposits (Fig. 1a).

The mechanical properties of PILP droplets were determined from *in situ* force curves (Fig. 2a and b). Two types of curves were observed, with the first type corresponding to periods before approximately 3 h, and the second type corresponding

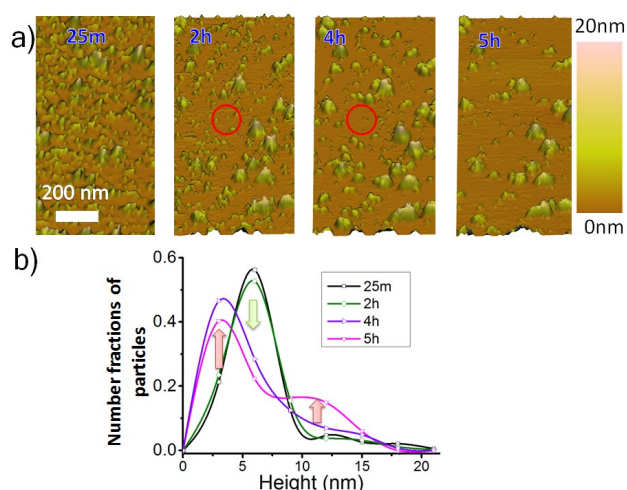


Fig. 1 The evolution of PILP deposits. (a) *In situ* AFM images over time. The red circles show the disappearance of small PILP adsorbates. (b) The height distribution of PILP deposits over time demonstrate a bimodal pattern, with one peak in height diminishing in size and shifting towards smaller dimensions, while the other peak grows in size, quantifying an Ostwald ripening process.

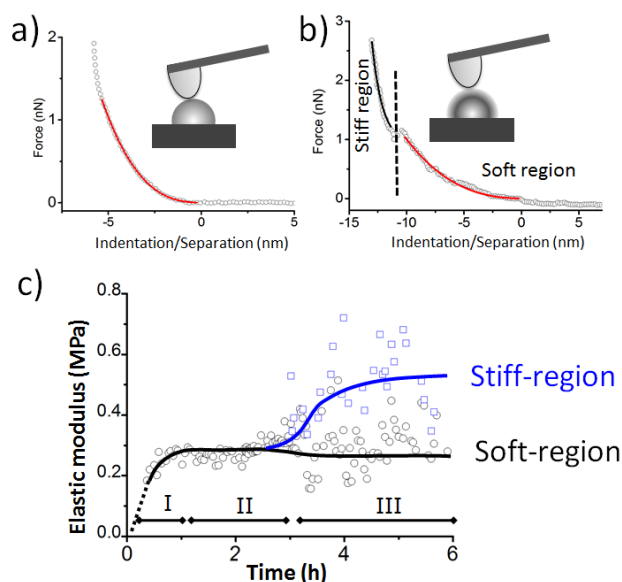


Fig. 2 Analysis of indentation force curves by using a modified Hertz model. The force versus distance of the PILPs and the corresponding fitted curve are presented, for (a) at initial stages (less than 2 h) and (b) at later stages (after 3 h), among which the fitted of the curve using a stiff/soft two-phase model in (b). (c) The changing elastic modulus of PILPs with time.

to later times. During the initial stages, the applied force exhibited a continuous increase with compression (Fig. 2a). However, the force curves collected at later time periods exhibited an abrupt, transient decline in applied force during the compression phase, followed by a sharp increase surpassing the previous force level (Fig. 2b).

To interpret these force curves, we examined two theoretical models for PILP behaviour. In one model, PILP is regarded as an elastic solid, while in the other, it is considered as a liquid droplet. For the former case, a Hertzian model is commonly employed for analyzing indentation by a conical tip;¹⁷ however, for a thin material on a hard substrate, a modified Hertzian model is deemed a more suitable choice¹⁸ and provides a better fit to the force curves (see Fig. S3, ESI†). Application of this model results in an elastic modulus for PILP that gradually increases from about 0.18 MPa to about 0.28 MPa between 25 min and 1 h (Fig. 2c). Extrapolation of the data back through the period where data collection was not feasible at the beginning of the experiment suggests that the modulus approaches a very small value — close to zero, suggesting that PILP initially behaves as a true liquid phase.

Once the modulus reached 0.28 MPa, it remained stable for approximately 2 h. At about 3 h, the sudden drop in force with compression in subsequent force curves indicated the occurrence of an additional yield point (Fig. 2b), signifying partial structural collapse. However, with further indentation, the material re-strengthened. This behaviour implies the presence of two distinct regions within the material, characterized by differing levels of softness and stiffness. The stiff region may have been formed due to the expulsion of PAA and/or H₂O, as has been seen in the core-shell particles (and helices) formed via PILP phases.^{19, 20} By incorporating a soft region and a stiff region in the modified Hertzian model, the elastic modulus of both periods of behaviour can be ascertained from the force curves (see Fig. 2c and Supported text, ESI†). In the stiff region, the modulus gradually increases over time to about 0.52 MPa, whereas in the soft region, the modulus remains mostly constant with a slight decrease to about 0.27 MPa (Fig. 2c). Our *in situ* FTIR characterization of the particles in

solution revealed the appearance of the carboxylate peak of PAA at 1640 cm⁻¹ during the later stage (i.e. just before the crystallization of vaterite) (Fig. S4, ESI†),^{21, 22} indicating the expulsion of PAA in the outer region of the particle and thereby reinforcing the interpretation of the force curves.

Despite the above analysis giving a reasonable result, it is essential to contemplate the prospect that PILP behaves as a genuine liquid, with its resistance to deformation stemming from the high interfacial tension between the PILP and the surrounding solution, rather than a quantifiable elastic modulus. As a droplet undergoes deformation when pressed against an AFM probe during a force measurement, the surface area increases, consequently augmenting the total interfacial free energy. Assuming that the rise in total interfacial free energy equates to the external work of compression by the AFM probe, the interfacial tension can be estimated by fitting the model to the recorded force curves (see Fig. 3a and supported text, ESI†). This analysis suggests that the initial interfacial tension should be approximately 350 mJ/m² (Fig. 3b), dropping to around 40 mJ/m² after 3 h. In this model, the excluded PAA could act as a surfactant to reduce the interfacial tension at a later stage.

The intrinsic nature of PILP may be positioned between two

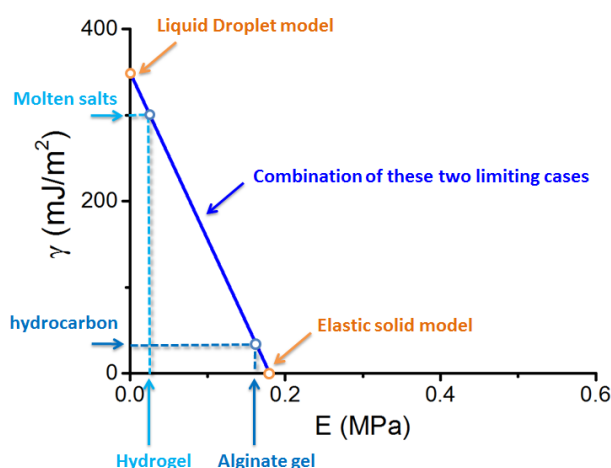


Fig. 4 The interfacial and mechanical properties of PILP considering the combination of a liquid and an elastic material.

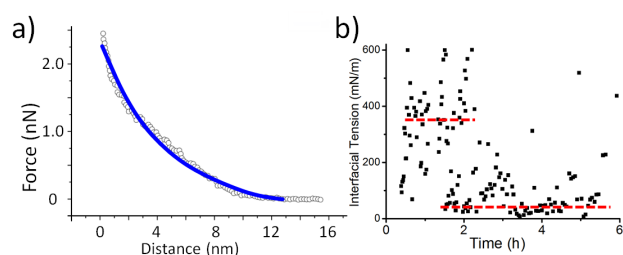


Fig. 3 Analysis of indentation force curves by using the model of deformed droplets. (a) The force versus distance of the PILPs and the corresponding fitted curve are presented. (b) The evolving interfacial tension of PILPs. The mean values of the interfacial tension are 350 and 40 mJ/m² for the initial phase (less than 2 h) and the later phase (more than 3 h), respectively, where the red dashed lines are drawn as a guide.

limited cases, i.e., a deformable solid with a minor elastic modulus (gel-like amorphous precursor²³) or a true liquid (liquid-like precursor²⁴) with a high interfacial energy. Since both the elastic modulus and the interfacial tension estimated from the data are proportional to the measured force (see Eqs. (1) and (13) in the supported text, ESI†), their values for any intermediate case would then be determined by a linear interpolation between the two limiting values, as shown in Fig. 4. Consequently, the elastic modulus of early PILP lies between 0 and 0.18 MPa, while the surface tension ranges from 350 to 0 mJ/m². If the surface tension of PILP resembles that of molten salts (e.g. CaF₂/air, 300 mJ/m²; sulfide/silicate, 500 mJ/m²),^{25, 26} which are also ion-rich phases, then the interpolated elastic modulus value must be small, around 0.03 MPa, or close to that

of a hydrogel. Conversely, if the surface tension of PILP is low, similar to that of silicone oil or hydrocarbons, about 40 mJ/m^2 ,²⁷ then the interpolated elastic modulus value is about 0.16 MPa, or close to that of alginate or double network gels.^{28, 29} Considering the precursor's composition of water, ions, and charged polyelectrolyte, it is probable that the interfacial tension would exceed the lower limit of a hydrocarbon, suggesting an intermediate value softer than an alginate gel. In either limiting case, a fluid with a high interfacial energy, such as a molten salt, or a soft gel-like material with a low elastic modulus, would be readily mouldable. Liquid properties would be required for a material that infiltrates nanoscale compartments in macromolecular matrices via capillary forces, and thus this aspect could only occur in the early stages of fluidic properties, or with greater stabilization of the liquid-like phase (potentially influenced by the polymer properties, such as molecular weight or charge density).³⁰ Consequently, our findings support the hypothesis that PILP represents a mouldable precursor, and are not inconsistent with an initial liquid state capable of infiltrating matrices prior to gelation and solidification. The increase in modulus over time suggests that the PILP droplets may become gel-like by the time they accumulate into a film or monolithic phase, which could account for the remnant colloidal texture observed in crystal products formed by the PILP process. Thus, the distance and time involved in various transport pathways — whether in the beaker or an organism — would be expected to lead to variations in the coalescence capability of such a precursor phase. Furthermore, polymers in and of themselves tend to possess strong viscoelastic behaviour, and thus likely contribute to the time-dependent behaviour of the PILP phase, thereby enabling the colloid assembly and transformation (CAT) pathway that provides such inimitable mineralization capabilities.¹⁶

We thank Dr. Stefano Cabrini, Dominik Ziegler, and Kai Chen for FIB assistance, and Dr. Virginia Altoe for SEM assistance. This work was supported by the National Science Foundation for Young Scientists of China (Grant No. 22205202), and the National Natural Science Foundation of China (Grant No. 22077114). This material is based in part on previous work supported by the National Science Foundation (Grant No. DMR-0710605). This research was performed at the Molecular Foundry, Lawrence Berkeley National Laboratory, which is supported by the Office of Basic Energy Sciences, Scientific User Facilities Division under Contract No. DE-AC02-05CH11231, and at the Pacific Northwest National Laboratory, a multi-program national laboratory operated for the Department of Energy by Battelle under Contract No. DE-AC05-76RL01830.

Conflicts of interest

There are no conflicts to declare.

Notes and references

- W. J. Habraken, J. Tao, L. J. Brylka, H. Friedrich, L. Bertinetti, A. S. Schenk, A. Verch, V. Dmitrovic, P. H. H. Bomans, P. M. Frederik, J. Laven, P. van der Schoot, B. Aichmayer, G. de With, J. J. DeYoreo and N. A. J. M. Sommerdijk, *Nat. Commun.*, 2013, **4**, 1507.
- B. Jin, Y. Chen, J. Tao, K. J. Lachowski, M. E. Bowden, Z. Zhang, L. D. Pozzo, N. M. Washton, K. T. Mueller and J. J. De Yoreo, *Angew. Chem. Int. Ed.*, 2023, e202303770.
- T. A. Grünewald, S. Checchia, H. Dicko, G. Le Moullac, M. Sham Koua, J. Vidal-Dupiol, J. Duboisset, J. Nouet, O. Grauby, M. Di Michiel and V. Chamard, *Proc. Natl. Acad. Sci. U. S. A.*, 2022, **119**, e2212616119.
- G. M. Zhu, M. L. Sushko, J. S. Loring, B. A. Legg, M. Song, J. A. Soltis, X. Huang, K. M. Rosso and J. J. De Yoreo, *Nature*, 2021, **590**, 416-422.
- Y. Wang, S. Xue, Q. Lin, D. Song, Y. He, L. Liu, J. Zhou, M. Zong, J. J. De Yoreo, J. Zhu, K. M. Rosso, M. L. Sushko and X. Zhang, *Proc. Natl. Acad. Sci. U. S. A.*, 2022, **119**, e2112679119.
- J. T. Avaro, S. L. P. Wolf, K. Hauser and D. Gebauer, *Angew. Chem. Int. Ed.*, 2020, **59**, 6155-6159.
- L. B. Gower and D. J. Odum, *J. Cryst. Growth*, 2000, **210**, 719-734.
- M. J. Olszta, X. Cheng, S. S. Jee, R. Kumar, Y. Y. Kim, M. J. Kaufman, E. P. Douglas and L. B. Gower, *Mater. Sci. Eng. R.*, 2007, **58**, 77-116.
- S. J. Homeijer, M. J. Olszta, R. A. Barrett and L. B. Gower, *J. Cryst. Growth*, 2008, **310**, 2938-2945.
- S. J. Homeijer, R. A. Barrett and L. B. Gower, *Cryst. Growth Des.*, 2010, **10**, 1040-1052.
- Y. F. Xu, K. C. H. Tijssen, P. H. H. Bomans, A. Akiva, H. Friedrich, A. P. M. Kentgens and N. A. J. M. Sommerdijk, *Nat. Commun.*, 2018, **9**, 2582.
- A. S. Schenk, H. Zope, Y.-Y. Kim, A. Kros, N. A. J. M. Sommerdijk and F. C. Meldrum, *Faraday Discuss.*, 2012, **159**, 327-344.
- F. F. Amos, D. M. Sharbaugh, D. R. Talham, L. B. Gower, M. Fricke and D. Volkmer, *Langmuir*, 2007, **23**, 1988-1994.
- F. Nudelman, K. Pieterse, A. George, P. H. H. Bomans, H. Friedrich, L. J. Brylka, P. A. J. Hilbers, G. de With and N. A. J. M. Sommerdijk, *Nat. Mater.*, 2010, **9**, 1004-1009.
- M. A. Bewernitz, D. Gebauer, J. Long, H. Cölfen and L. B. Gower, *Faraday Discuss.*, 2012, **159**, 291-312.
- L. Gower and J. Elias, *J. Struct. Biol.: X*, 2022, **6**, 100059.
- H. Hertz, *J. Reine Angew. Math.*, 1881, **92**, 156-171.
- E. K. Dimitriadis, F. Horkay, J. Maresca, B. Kachar and R. S. Chadwick, *Biophys. J.*, 2002, **82**, 2798-2810.
- L. Dai, X. Cheng and L. B. Gower, *Chem. Mater.*, 2008, **20**, 6917-6928.
- L. Dai, E. P. Douglas and L. B. Gower, *J. Non-Cryst. Solids*, 2008, **354**, 1845-1854.
- A. Sarac, B. Ustamehmetoglu and H. Yildirim, *J. Appl. Polym. Sci.*, 2002, **84**, 723-728.
- S. Dubinsky, G. S. Grader, G. E. Shter and M. S. Silverstein, *Polym. Degrad. Stab.*, 2004, **86**, 171-178.
- S. L. P. Wolf, L. Caballero, F. Melo and H. Cölfen, *Langmuir*, 2017, **33**, 158-163.
- M. B. Gindele, S. Nolte, K. M. Stock, K. Keibel and D. Gebauer, *Adv. Mater.*, 2023, **35**, 2300702.
- X. Chen, S. Jinguu, S. Nishimura, Y. Oyama and K. Terashima, *J. Cryst. Growth* 2002, **240**, 445-453.
- J. E. Mungall and S. Su, *Earth Planet. Sci. Lett.*, 2005, **234**, 135-149.
- F. Peters and D. Arabali, *Colloids Surf. A*, 2013, **426**, 1-5.
- A. Miserez, J. C. Weaver and O. Chaudhuri, *J. Mater. Chem. B*, 2015, **3**, 13-24.
- J. Li, Z. Suo and J. J. Vlassak, *J. Mater. Chem. B* 2014, **2**, 6708-6713.
- T. T. Thula, F. Svedlund, D. E. Rodriguez, J. Podschun, L. Pendi and L. B. Gower, *Polymers*, 2010, **3**, 10-35.